

## $^{15}\text{N}$ – $^1\text{H}$ Scalar Coupling Perturbation: An Additional Probe for Measuring Structural Changes Due to Ligand Binding

Junhe Ma, James M. Gruschus, and Nico Tjandra\*

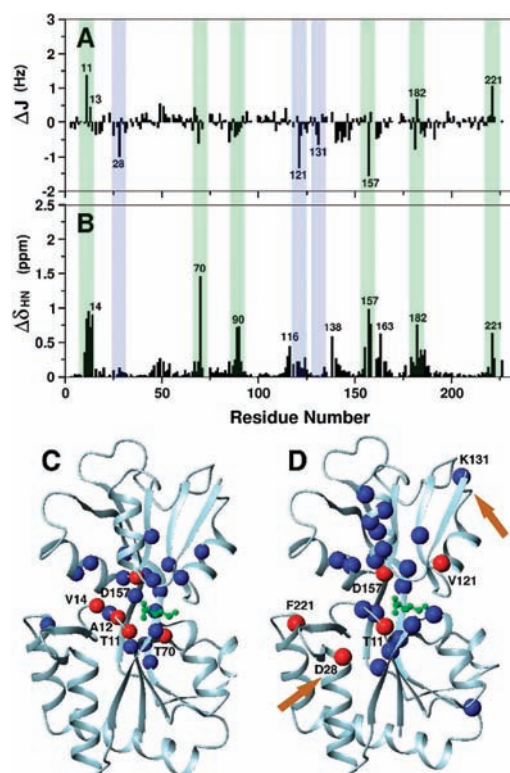
Laboratory of Molecular Biophysics, National Heart, Lung, and Blood Institute, National Institutes of Health, 50 South Drive, Bethesda, Maryland 20892

Received May 1, 2009; E-mail: tjandran@nhlbi.nih.gov

Chemical shift perturbation mapping of backbone amides is one of the most widely employed techniques in biomolecular NMR.<sup>1,2</sup> It provides residue-by-residue information on interaction interfaces, ligand binding, and chemical modification sites. It is applicable even for samples where poor solubility, short lifetime, or large size precludes more sophisticated experimental approaches. Here, we show that significant changes can also occur in the backbone amide  $^{15}\text{N}$ – $^1\text{H}$  scalar coupling constants for glutamine binding protein (GlnBP) due to ligand binding. Like chemical shift perturbations, large changes ( $>1$  Hz) are seen near the site of glutamine binding, though perturbations also occur distant to the site. The coupling constant perturbations correlate with significant structural changes, especially changes in backbone hydrogen bonding.<sup>3–6</sup> More importantly some of the changes in the  $J$ -couplings do not correspond to changes in the chemical shifts. Thus, amide scalar coupling perturbation can serve as an adjunct to chemical shift perturbation, providing additional information on both short-range and longer-range, allosteric structural changes.

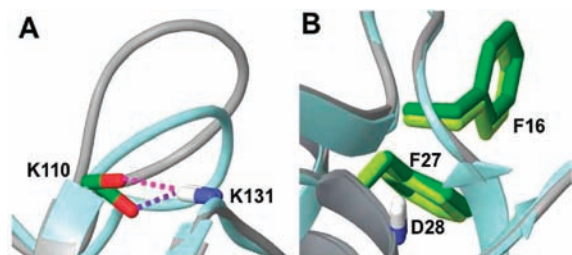
Nuclear spin–spin scalar coupling between nuclei is relayed via their interactions with the electrons of the system.<sup>7</sup> The interaction is dominated by the four Ramsey terms, the diamagnetic and paramagnetic spin–orbit, spin–dipole, and Fermi contact mechanisms.<sup>8</sup> The first two, diamagnetic and paramagnetic spin–orbit mechanisms, are related to the diamagnetic and paramagnetic shielding terms that lead to chemical shift perturbation, thus the perturbation in coupling values arising from these terms should resemble the pattern seen for chemical shift perturbation. The second two terms have no shielding counterparts, and for one-bond scalar coupling, the Fermi contact term dominates. The largest contribution arises from  $s$ -orbital spin density centered at one nucleus overlapping with the coupled nucleus and thus has a strong dependence on bond length. The HN bond length depends, in turn, on its immediate electronic environment, on hydrogen bonding in particular.<sup>9,10</sup>

Figure 1A and 1B compare plots of the HN scalar coupling ( $\Delta J_{\text{HN}}$ ) and the weighted average chemical shift differences ( $\Delta\delta_{\text{HN}}$ , calculated by equation, i.e.,  $\{[(\Delta H)^2 + (\Delta N/5)^2]/2\}^{1/2}$ )<sup>11,12</sup> between the bound and the free form GlnBP. Figure 1C and 1D compare the largest chemical shift and  $J$ -coupling changes mapped onto the glutamine-bound GlnBP structure.<sup>13b</sup> The coupling constant perturbations are more dispersed through the structure compared to the chemical shift changes. Two among the top five  $\Delta J_{\text{HN}}$  values, D157 ( $-1.6$  Hz) and T11 (1.4 Hz), correspond to two of the largest chemical shift changes, and both lie adjacent to the bound glutamine. Three of the top five  $\Delta J_{\text{HN}}$ , T11, V121 ( $-1.3$  Hz), and D157, undergo formation or breaking of hydrogen bonds upon ligand binding. Overall, the  $J$ -coupling changes for amides undergoing hydrogen bond breakage or formation are twice as large ( $\pm 0.5$  Hz) as those which remain bonded ( $\pm 0.25$  Hz). Also notable is K131 ( $\Delta J_{\text{HN}}$  0.7 Hz), which lies adjacent to one of the most



**Figure 1.** NMR-observed scalar coupling difference (A) and the weighted average chemical shift differences profile (B) of GlnBP<sup>13</sup> between bound and free form. Residues with significant  $J$ -coupling and backbone amide chemical shift change are shaded green, while the residues with only significant  $J$ -coupling changes are shaded blue. The absence of a bar indicates the presence of a proline or a residue that is overlapped. 25 residues exhibiting the largest chemical shift and  $J$ -coupling changes are mapped onto the glutamine-bound structure of GlnBP<sup>13b</sup> shown in images C and D, respectively. The top five residues with the largest chemical shift and  $J$ -coupling changes are colored red and the rest are colored blue; the figure was created with the program MOLMOL.<sup>14</sup> Residues D28 and K131 are denoted by the dark orange arrows. All NMR data shown here were recorded for 1.2 mM protein/substrate at 41 °C on a Bruker Avance 800 MHz spectrometer equipped with a cryoprobe and Z pulse field gradient.

structurally labile loops of the GlnBP protein (Figure 2A). Backbone amide residual dipolar couplings (RDCs) predicted from the X-ray structures show poor agreement with the measured RDC values for this region (data not shown); thus Figure 2A might underrepresent the structural changes in solution for K131. One of the largest coupling constant perturbations appears unrelated to hydrogen bonding, that of Asp28 ( $\Delta J_{\text{HN}}$   $-1.0$  Hz). This amide lies near two aromatic rings ( $<4$  Å), Phe16 and Phe27, illustrating the significance of the paramagnetic spin–orbit Ramsey term to the coupling constant perturbation (Figure 2B).



**Figure 2.** Expanded small region of superimposed free<sup>13a</sup> (PDB code 1GGG, colored gray) and bound<sup>13b</sup> (PDB code 1WDN, colored light blue) crystal structure of GlnBP around residues K131 (A) and D28 (B). The hydrogen bonding of residue K131 in the bound form is shown in purple while the free form is shown in pink. The aromatic rings of F16 and F27 around residue D28 in bound and free form are colored dark and light green, respectively.

The  $\Delta J_{\text{HN}}$  values shown in Figure 1 were obtained using the NMR signal intensity based  $J$ -modulation technique for greater accuracy. By this approach the interference effect arising from dipole/dipole cross-correlated relaxation is almost eliminated by refocusing spin evolution.<sup>15,16</sup> Repeated measurements indicated these values were reproducible to less than 0.08 Hz. Residues with significant resonance overlap were excluded from the analysis. The  $J$ -modulation experiments were repeated on a 600 MHz spectrometer, and the resulting  $\Delta J_{\text{HN}}$  values matched the 800 MHz results with a standard deviation of 0.15 Hz, providing an estimate of the accuracy of the technique. For comparison,  $\Delta J_{\text{HN}}$  values were also measured at 800 MHz using the in-phase and antiphase IPAP technique,<sup>17</sup> yielding a standard deviation of 0.20 Hz compared to the 800 MHz  $J$ -modulation values. The larger deviation reflects dipole–dipole cross-correlated relaxation and unresolved E.COSY effects.<sup>18</sup> The spread in  $\Delta J_{\text{HN}}$  values seen for GlnBP is  $-1.6$  to  $1.4$  Hz, so the IPAP technique should be adequate for identifying large  $\Delta J_{\text{HN}}$  values, while the  $J$ -modulation experiment will be needed for detecting more subtle perturbations near 0.2 Hz.

Measurement of free GlnBP  $\Delta J_{\text{HN}}$  values at two salt concentrations (0 and 100 mM NaCl) showed no significant changes ( $\pm 0.07$  Hz), and the  $\Delta J_{\text{HN}}$  values for free GlnBP showed no significant changes ( $\pm 0.07$  Hz) in the presence of a nonbinding substrate analogue, D-glutamic acid (1.2 mM). Comparison of  $\Delta J_{\text{HN}}$  values at two temperatures (31 and 41 °C) showed a slight increase (0.08 Hz) on average at the lower temperature, as expected from the relation between molecular tumbling correlation time and the dynamic frequency shift,<sup>19</sup> but showed no significant changes when the overall increase was subtracted (see the Supporting Information).

The differences in  $J$ -coupling and chemical shift changes (Figure 1A and 1B) suggest their values have different sensitivities to local perturbations despite sharing some very similar interaction terms in their Hamiltonians. Moreover these changes vary in sign depending on the local geometry. Even in cases where the dominant terms leading to perturbation are the same for both  $J$ -coupling and chemical shift, the various contributions to the chemical shift might cancel, while the contributions to the  $J$ -coupling might add, and *vice versa*. Thus, while it is natural to suspect that the  $J$ -couplings and chemical shifts will be perturbed similarly upon a conformational change, it is not surprising to find discrepancies.

Comparison of  $\Delta J_{\text{HN}}$  with  $^1\text{H}$  and  $^{15}\text{N}$  chemical shift differences reveals modest correlations, with a coefficient of 0.44 between  $\Delta J_{\text{HN}}$  and  $\Delta\text{N}$  and  $-0.31$  between  $\Delta J_{\text{HN}}$  and  $\Delta\text{H}$ . The magnitude of

changes for  $|\Delta J_{\text{HN}}|$  and  $\Delta\delta_{\text{HN}}$  (Figure 1B) also show some correlation (0.40), comparable to the correlation seen between  $|\Delta\text{H}|$  and  $|\Delta\text{N}|$  (0.46). No correlation was seen between either  $|\Delta J_{\text{HN}}|$  or  $\Delta\delta_{\text{HN}}$  and the backbone rms deviation between free and bound X-ray structures. Attempts to compare  $\Delta J_{\text{HN}}$  to linear combinations of backbone ( $\varphi$ ,  $\psi$ ,  $\omega$ ) and side chain ( $\chi_1$ ,  $\chi_2$ ) dihedral angles also produced no significant correlations. Even with hydrogen bond length and angle information included, no simple correlation was seen. This concurs with calculations of  $\Delta J_{\text{HN}}$  using *ab initio* density functional theory which predict that the sign of the variation of  $\Delta J_{\text{HN}}$  as a function of hydrogen bond length depends also on other variables, such as HCO angle.<sup>9</sup> Thus, HN coupling constant perturbations provide valuable information on where structural changes occur but do not reveal what specifically those structural changes are.

On a final note, the results here also represent a cautionary message. When determining changes in residual dipolar couplings, between free and bound states, for instance, changes in the isotropic HN  $J$ -coupling constants must be taken into account as well. This also applies to residual dipolar couplings of minor population states deduced through  $R_2$  dispersion techniques.<sup>20</sup>

**Acknowledgment.** This work was supported by the Intramural Research Program of the NIH, National Heart, Lung, and Blood Institute.

**Supporting Information Available:** Correlation plot between  $J$ -coupling and chemical shift differences for GlnBP; Chemical shift and  $J$ -coupling changes mapped onto the glutamine-free structure of GlnBP;  $J$ -coupling at two temperatures; salt and nonbinding amino acid dependence; table of  $J$ -coupling values of bound and free GlnBP. This material is available free of charge via the Internet at <http://pubs.acs.org>.

## References

- (1) Farmer, B. T.; Constantine, K. L.; Goldfarb, V.; Friedrichs, M. S.; Wittekind, M.; Yanchunas, J.; Robertson, J. G.; Mueller, L. *Nat. Struct. Biol.* **1996**, *3*, 995–997.
- (2) Williamson, R. A.; Carr, M. D.; Frenkiel, T. A.; Feeney, J.; Freedman, R. B. *Biochemistry* **1997**, *36*, 13882–13889.
- (3) Blake, P. R.; Park, J.-B.; Adams, M. W.; Summers, M. F. *J. Am. Chem. Soc.* **1992**, *114*, 4931–4933.
- (4) Cordier, F.; Grzesiek, S. *J. Am. Chem. Soc.* **1999**, *121*, 1601–1602.
- (5) Cordier, F.; Barfield, M.; Grzesiek, S. *J. Am. Chem. Soc.* **2003**, *125*, 15750–15751.
- (6) Bouvignies, G.; Bernado, P.; Meier, S.; Cho, K.; Grzesiek, S.; Brueschweiler, R.; Blackledge, M. *Proc. Natl. Acad. Sci. U.S.A.* **2005**, *102*, 13885–13890.
- (7) Helgaker, T.; Watson, M.; Handy, N. C. *J. Chem. Phys.* **2000**, *113*, 9402–9409.
- (8) Ramsey, N. F.; Purcell, E. M. *Phys. Rev.* **1952**, *85*, 143–144.
- (9) Tuttle, T.; Kraka, E.; Wu, A. A.; Cremer, D. *J. Am. Chem. Soc.* **2004**, *126*, 5093–5107.
- (10) Sahakyan, A. B.; Shakhmatuni, A. G.; Shakhmatuni, A. A.; Panosyan, H. A. *J. Phys. Chem. A* **2008**, *112*, 3576–3586.
- (11) Garrett, D. S.; Seok, Y. J.; Peterkofsky, A.; Clore, G. M.; Gronenborn, A. M. *Biochemistry* **1997**, *36*, 4393–4398.
- (12) Chen, K.; Bachtar, I.; Piszczek, G.; Bouamr, F.; Carter, C.; Tjandra, N. *Biochemistry* **2008**, *47*, 1928–1937.
- (13) (a) Hsiao, C. D.; Sun, Y. J.; Rose, J.; Wang, B. C. *J. Mol. Biol.* **1996**, *262*, 225–242. (b) Sun, Y. J.; Rose, J.; Wang, B. C.; Hsiao, C. D. *J. Mol. Biol.* **1998**, *278*, 219–229.
- (14) Koradi, R.; Billeter, M.; Wüthrich, K. *J. Mol. Graphics* **1996**, *14*, 51–55.
- (15) de Alba, E.; Tjandra, N. *J. Magn. Reson.* **2006**, *183*, 160–165.
- (16) de Alba, E.; Tjandra, N. *J. Biomol. NMR* **2006**, *35*, 1–16.
- (17) Ottiger, M.; Delaglio, F.; Bax, A. *J. Magn. Reson.* **1998**, *131*, 373–378.
- (18) Yao, L.; Ying, J.; Bax, A. *J. Biomol. NMR* **2009**, *43*, 161–170.
- (19) Tjandra, N.; Grzesiek, S.; Bax, A. *J. Am. Chem. Soc.* **1996**, *118*, 6264–6272.
- (20) Vallurupalli, P.; Hansen, D. F.; Kay, L. E. *Proc. Natl. Acad. Sci. U.S.A.* **2008**, *105*, 11766–11771.

JA903552Q